

Geert-Jan L.M. de Haas · Timo G. Nijland
Peter J. Valbracht · Cees Maijer · Rob Verschure
Tom Andersen

Magmatic versus metamorphic origin of olivine-plagioclase coronas

Received: 5 April 2001 / Accepted: 17 February 2002 / Published online: 31 May 2002
© Springer-Verlag 2002

Abstract An SEM, REE, and mineral Sm–Nd isotope study on olivine-plagioclase coronas in the Vestre Dale gabbro, Norway, was carried out in order to solve the temporal relationships within these coronas. It is demonstrated that in contrast to common models, corona formation is a multistage, late-magmatic process, starting with the formation of orthopyroxene by (partial) dissolution of olivine, followed by the nucleation and rapid outward growth of orthopyroxene + spinel symplectites at its outer margin, and concluded by replacement of this precursory outer shell by calcic amphibole. Isotopic equilibrium between inner shell orthopyroxene

and the magmatic assemblage, and the REE contents of orthopyroxene and outer shell amphibole also provide strong arguments for a magmatic origin, with the local availability of fractionated magma acting as a limiting factor. The absence of replacement of intercumulus clinopyroxene by amphibole also favours a late stage magmatic rather than a metamorphic origin for corona amphibole.

Introduction

Coronitic microstructures have been documented in both metamorphic and igneous rocks (e.g. Bard 1986). They record reactions between previously bordering minerals in response to changing physico-chemical conditions. Such reactions involve (partial) consumption of the neighbouring minerals and the growth of new minerals at the former interface between these minerals. A well-known example of coronitic microstructures in magmatic rocks are plagioclase-olivine coronas. In most cases, the corona consists of an inner shell of orthopyroxene around olivine, rimmed by clinopyroxene and/or amphibole and a clinopyroxene and/or amphibole + spinel symplectite. In some cases, an outermost shell of garnet or, more rarely, biotite may be present.

These structures have first been described by Törnebohm (1877) from the Lake Vänern area in Sweden, soon followed by several descriptions from the Bamble area (e.g. Sjögren 1883). W.C. Brögger, in his lectures in Stockholm in April 1885, coined the term ‘coronas’, also used subsequently by Lacroix (1889, ‘couronnes’). Rosenbusch (1910) then created confusion by grouping them together with kelyphitic rims, denominating them ‘Ozellarstruktur oder kelyphitische Struktur’ (Rosenbusch 1910, p. 178), although the latter, first denominated by Schrauf (1882), have a different structure and, as recognised early, origin (Sederholm 1916; Brögger 1934). From these times, proponents of a secondary, metamorphic origin (e.g. Törnebohm 1877; Becke 1882; Lacroix

G.-J.L.M. de Haas (✉) · T. Andersen
Laboratorium for isotopgeologi,
Mineralogisk-Geologisk Museum,
Sars'gate 1, 0562 Oslo, Norway
E-mail: geert-jan.dehaas@geo.ntnu.no

T.G. Nijland
Roosevelttlaan 964,
3526 BP Utrecht, The Netherlands

P.J. Valbracht · R. Verschure
Institute of Earth Sciences,
Free University, De Boelelaan 1085,
1081 HV Amsterdam, The Netherlands

C. Maijer
Department of Geochemistry,
Utrecht University, P.O. Box 80021,
3508 TA Utrecht, The Netherlands

Present address: G.-J.L.M. de Haas
Institutt for geologi og bergteknikk,
NTNU, A. Getzvei 2, 7491 Trondheim, Norway

Present address: P.J. Valbracht
Fugro Inpark, Dillenburgsingel 69,
2260 DA Leidschendam, The Netherlands

Present address: R. Verschure
Verschure Geologix, Brahmssstraat 8,
1077 HH Amsterdam, The Netherlands

Present address: C. Maijer
Muntstraat 30,
3961 AL Wijk bij Duurstede, The Netherlands

Editorial responsibility: J. Touret

1889) and a primary, magmatic origin (e.g. Adams 1893) have exchanged views, whilst soon the involvement of deuteritic (metasomatic) fluids was proposed in combination with a secondary, metamorphic origin (Sederholm 1916), later elaborated in general by Korshinskij (1959).

Olivine-plagioclase coronas are a typical feature of medium- to high-pressure, amphibolite-granulite facies metamorphic terrains (e.g. Gardner and Robins 1974; Grieve and Gittins 1975; Grant 1988; Dam 1995), although Turner and Stuewe (1992) describe olivine-plagioclase coronas which have formed at a pressure of 1 kbar. As already stated, they have since long been known from the Bamble sector, southern Norway, first reported from the Ødegården gabbro by Sjögren (1883). Benchmark studies by Lacroix (1889) and Brøgger (1934) were followed by many studies on similar intrusions ('hyperites') in the area (e.g. Reynolds and Frederickson 1962; Frodesen 1968a, 1968b; Starmer 1969; Joesten 1986; Brickwood and Craig 1987; de Haas 1992; de Haas et al. 1992, 1993; Dam 1995).

From Bugge (1943) onwards, solid-state or fluid-assisted metamorphic processes became the most commonly proposed mechanism for corona development in Bamble coronitic gabbros. According to Bugge (1943), the coronas formed through a solid-state reaction, in connection with magmatic processes. Frodesen (1968a) proposed a combined deuterio-magmatic metamorphic origin whereas Reynolds and Frederickson (1962) and Morton et al. (1970) related corona growth to subsequent introduction of silica-bearing solutions. Starmer (1969) suggested that the coronas started to grow early in the cooling history and continued to develop in response to isobaric cooling at elevated pressures. In view of the apparent contrast between P-T conditions required for corona-forming reactions and the regional metamorphic conditions, Brickwood and Craig (1987) took a similar view. Dam (1995) obtained temperatures in the order of 825 °C for coronitic assemblages in samples from the Vestre Dale gabbro, and therefore regarded the coronas as cooling-related phenomena.

A solid-state, subsolidus origin of the coronas and formation during the initial stages of cooling of an intrusion were also proposed in other terrains, and is currently agreed upon by most workers (e.g. Gardner and Robins 1974; Mongkoltip and Ashworth 1983; Grant 1988). This mechanism implies a single-stage origin for olivine-plagioclase coronas (Grant 1988; Ashworth et al. 1992), i.e. the individual layers formed simultaneously. By contrast, Joesten (1986) proposed a primary, magmatic origin for the olivine-plagioclase coronas. This model implies a multistage evolution of the coronas, in which an initial corona formed at the magmatic stage is modified by annealing and rearrangement, resulting in a stable sequence of mineral assemblages through the corona. This was disputed by Ashworth (1986), although he did not exclude the possibility that the reaction started very early in the cooling history, with some residual liquid still being present. Davidson and Van Breemen (1988), however, obtained

ages differing by as much as 125 Ma for baddeleyite and a surrounding corona of columnar zircon, and this corona was interpreted to be contemporaneous with the olivine-plagioclase corona. If this interpretation is correct, these results indicate a post-cooling origin for the latter, at least in the gabbro studied by these authors. However, the process of corona growth between plagioclase and olivine is rather complex, as is underlined by the observation of Nijland et al. (1996) that apparently stable plagioclase-olivine contacts and (recrystallised) coronitic microstructures may occur in a single thin section.

The results of a TEM study on the inner orthopyroxene shell of the Vestre Dale gabbro, south Norway, seem to indicate that a two-stage evolution of coronas can not be excluded (Dam 1995). These observations again impose the following questions.

1. Did all corona shells develop simultaneously (single-stage model), or was their growth separated in time (multistage model)?
2. Did the corona develop in response to magmatic evolution, physicochemical conditions imposed during regional metamorphism, or fluid infiltration?

In order to answer these questions, an Sm-Nd isotopic, SEM and REE study was performed on primary (plagioclase, olivine, clinopyroxene) and corona minerals (orthopyroxene, spinel, amphibole) in a sample from the Vestre Dale gabbro. We show that the answer to the first question is the multistage model, and that to the second question, at least as far as the orthopyroxene inner shell is concerned, is magmatic evolution. We present a model for corona development which not only supports concepts advocated earlier by Joesten (1986) but also revives the notions proposed by Hommel (1919) and Vogt (1921), i.e. development during magmatic cooling, under influence of changing compositions of interstitial liquids.

Geological setting

The Bamble sector, south Norway, forms part of the Southwest Scandinavian Domain of the Baltic Shield (Fig. 1) which was accreted and reworked during several mid-Proterozoic events. The Bamble sector is constituted by gneisses which were metamorphosed to the amphibolite/granulite facies during Sveconorwegian (1.25–0.95) and less well-defined pre-Sveconorwegian events (for a detailed account on the lithologies and the structural evolution of the Bamble sector, the reader is referred to Starmer 1985). Sveconorwegian P-T conditions range from 752 ± 34 °C and 7.1 ± 0.4 kbar for the amphibolite facies zone to 836 ± 49 °C and 7.7 ± 0.3 kbar for the granulite facies zone (Nijland and Maijer 1993). Kullerud and Dahlgren (1993) constrained the timing of Sveconorwegian peak-metamorphic conditions to the interval 1,152–1,095 Ma.

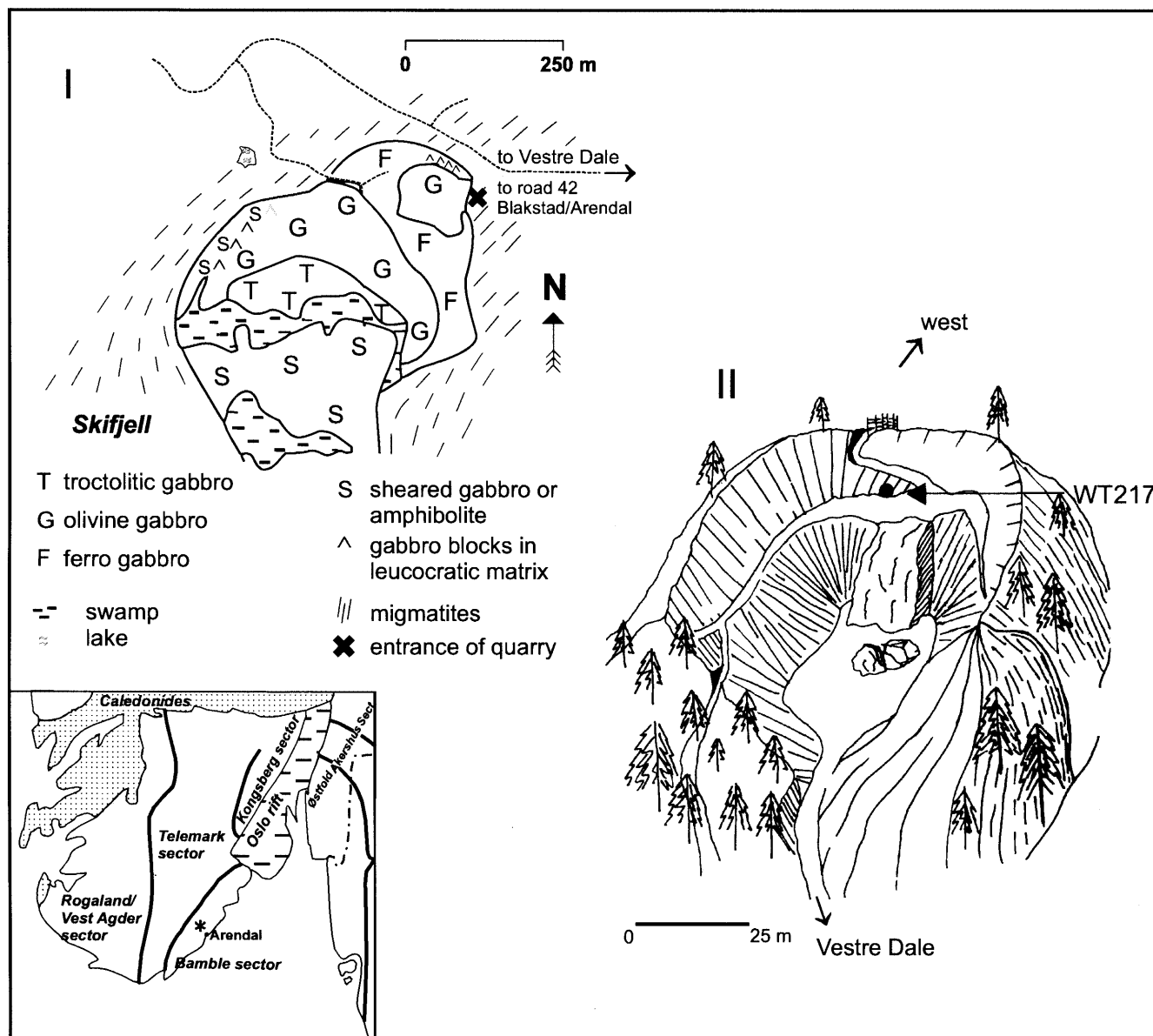


Fig. 1. Geological map of the Vestre Dale gabbro (I) and sketch of the Vestre Dale quarry with the location of sample WT217 (II). Inset shows the mid-Proterozoic Southwest Scandinavian Domain and its constituent segments (sectors)

The Vestre Dale gabbro is a lens-shaped body surrounded by migmatitic gneisses (Fig. 1), situated in the amphibolite facies part of the amphibolite-granulite transition zone. The gabbro has previously been dated by Sm–Nd whole-rock method at 1.11 ± 0.14 Ga (de Haas et al. 1992, 1993). The inner part of the outcrop consists of fine-grained, coronitic gabbro with purple plagioclase and greenish olivine. The grain size increases towards the contact where the gabbro displays a subophitic texture built up by cm-scale plagioclase and dark-green hornblende. The foliation in the locally migmatitic gneisses wraps around the gabbro. At the entrance of the quarry the gabbro-gneiss contact is subhorizontal. Just above the contact, dark, angular to subrounded gabbroic blocks float in a leucocratic matrix, constituting an agmatitic texture. The foliated parts of the gabbro are strongly amphibolitised along the contact. The southern extension consists of a strongly foliated garnet-amphibolite.

roic blocks float in a leucocratic matrix, constituting an agmatitic texture. The foliated parts of the gabbro are strongly amphibolitised along the contact. The southern extension consists of a strongly foliated garnet-amphibolite.

On a microscopic scale, a transition from troctolitic gabbro to olivine-rich and olivine-poor gabbro to ferro-gabbro is observed from the core of the intrusion towards the outer margin. The amount of olivine decreases from 65 modal% in the troctolitic gabbro to 40–25 modal% in the olivine gabbros. Olivine is absent in the ferro-gabbro. Cumulus plagioclase is concentrated in clusters, irregularly distributed in the olivine mesocumulate (terminology after Irvine 1982) which, in the case of the troctolitic gabbros, tends to evolve into an adcumulate. Clinopyroxene and ilmenite are intercumulus phases. Clinopyroxene contains three types of exsolution: (1) ilmenite flakes parallel to (100) and (001),

(2) segregated blebs of orthopyroxene with a length and width up to 145 and 20 μm respectively, and (3) exsolution lamellae of another pyroxene (?) with a width up to 2 μm . Type 2 exsolutions most likely represent migrated exsolution lamellae and predate type 3 exsolutions. Where intercumulus clinopyroxene is in contact with cumulus olivine, orthopyroxene of type 2 exsolutions seems to nucleate at the crystal face of olivine (Fig. 2). Coronas between olivine and plagioclase, and between ilmenite and plagioclase occur in the troctolitic and olivine gabbros. The inner rim of the olivine coronas consists of orthopyroxene whereas the outer rim is largely occupied by green amphibole (Fig. 3). Ilmenite coronas are mainly composed of brown amphibole, and sporadically contain minor biotite.

Parts of the clinopyroxene in the troctolitic and olivine gabbros display an irregular, thin rim of brown amphibole which locally has grown inwards along cleavage planes. By contrast, clinopyroxene in the ferrogabbros is bordered by granular aggregates of blue-green amphibole and quartz blebs. Late alteration includes the development of patchy or fibrous pale-green actinolite within intercumulus clinopyroxene in samples from the margin.

Objectives and sample selection

For the purpose of this study one olivine gabbro sample was selected. The sample, WT217 of de Haas et al. (1992), originates from the Vestre Dale quarry (Fig. 1), the best locality to study the Vestre Dale gabbro as it represents a continuous exposure of the transition from fresh, unaltered olivine gabbro in the core of the intrusion to the more evolved and altered ferrogabbro along the margin.

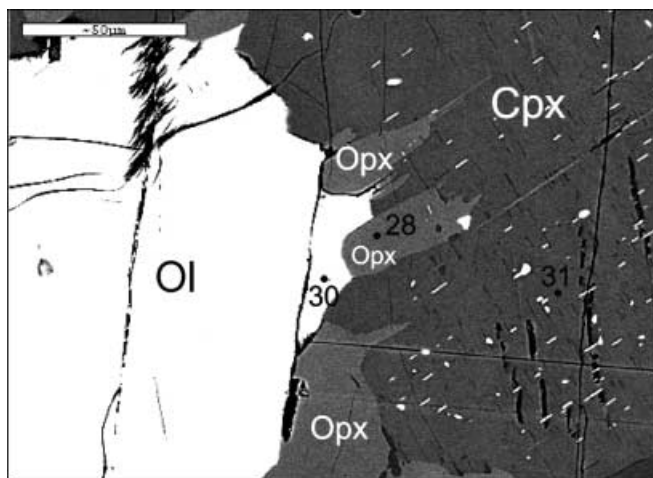


Fig. 2. Segregated blebs of type 2 orthopyroxene exsolution in intercumulus clinopyroxene, nucleated at the interface with cumulus olivine (numbers mark locality of microprobe analyses; see Table 1). *Ol* Olivine, *pl* plagioclase, *cpx* clinopyroxene, *opx* orthopyroxene, *am* amphibole, *spl* spinel, *bt* biotite

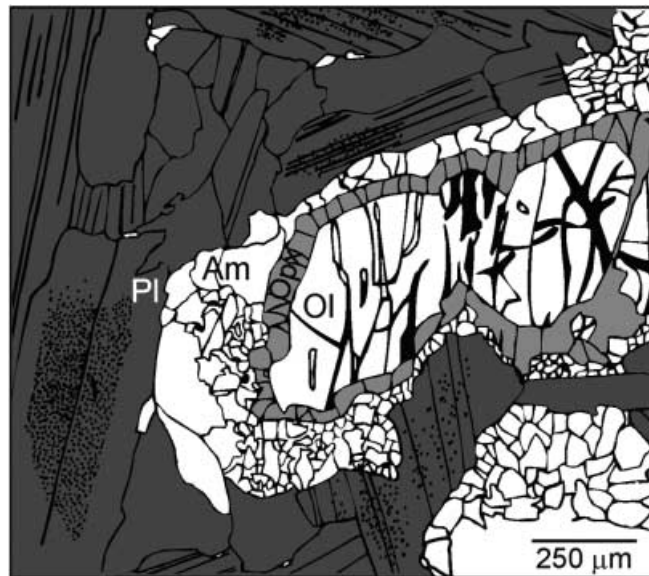


Fig. 3. Sketch of the olivine-plagioclase (dark shading) corona in Vestre Dale gabbro sample WT217, with an inner rim of orthopyroxene (light shading) and an outer rim of amphibole (for mineral abbreviations, see Fig. 2)

Olivine-plagioclase coronas were studied in great detail with SEM, supplemented with microprobe analyses. Special attention was paid to the spatial distribution of the corona minerals and contact relations between them. In addition, magmatic and corona minerals were analysed for their Sm–Nd isotope systematics in an attempt to resolve the temporal relation(s) between the magmatic assemblage and the corona mineralogy. More information about the processes which play a role in corona formation is provided by a modelling study applying the REE contents of the various minerals. It is demonstrated that the results allow for a further refinement of the model for corona formation.

Analytical techniques

Mineral analyses and SEM

Mineral compositions were determined at the Mineralogisk-Geologisk Museum, University of Oslo, with a Cameca Camebax electron microprobe, using natural and synthetic standards and Cameca's PAP software for online data reduction. Operating conditions were 15-kV acceleration voltage, 20-nA sample current, and 10-s counting time. Representative mineral analyses are listed in Table 1. SEM observations were performed with a JEOL JSM-840 scanning electron microscope at the Institutt for Geologi at Blindern, University of Oslo. Operating conditions were 15-kV accelerating voltage, 0.3-nA probe current, and 15-mm working distance.

Isotope and REE analyses

Ten kg of Vestre Dale gabbro sample WT217 was broken and crushed to grain sizes smaller than 250 μm . A split of ca. 75 g was

used for whole-rock analysis. Mineral separates for clinopyroxene, plagioclase, orthopyroxene, amphibole, and olivine were obtained by heavy-liquid and magnetic separation techniques. The plagioclase fraction was split into three density fractions by heavy liquid separation: 2.68–2.70 (I), 2.70–2.72 (II), and > 2.72 g/cm³ (III). The purity of the fractions was checked by XRD analysis. Final fractions were obtained by handpicking.

Sm–Nd isotope analyses were performed at the Laboratory for Isotope Geology, Free University, Amsterdam, according to the procedures described by Valbracht (1991). Sm and Nd mass spectrometry analyses were made using a Finnigan MAT 261 mass spectrometer with a fixed multicollector array. The very low Sm and Nd contents of olivine, 0.02 and 0.05 ppm respectively, did not allow for an accurate analysis of the isotopic composition. The results for the other minerals are listed in Table 2. Total Nd blanks were less than 1 ng. The ¹⁴³Nd/¹⁴⁴Nd ratios were normalised to ¹⁴⁶Nd/¹⁴⁴Nd = 0.7219. Three analyses of the La Jolla standard gave ¹⁴³Nd/¹⁴⁴Nd = 0.511853 ± 5 (2 s). Quoted errors in ¹⁴³Nd/¹⁴⁴Nd are within-run precision (1σ). The precision of the ¹⁴³Nd/¹⁴⁴Nd ratio is estimated to be 0.002%. The error in the ¹⁴⁷Sm/¹⁴⁴Nd ratios is generally less than 0.2%. Sm and Nd concentrations have an uncertainty of ca. 1.0% (cf. Valbracht 1991). Isochron calculations were performed using the Isoplot 2.90 software package (Ludwig 1996), using λ-¹⁴⁷Sm = 6.54 × 10⁻¹² a⁻¹. All calculated isochron errors are 2s.

REE analyses were made by INAA at the IRI in Delft according to the procedures described by de Bruin (1983). The precision is generally better than 10%. The results are listed in Table 2.

Petrographic and SEM observations on the corona structure

Olivine is unzoned with Fo contents of about 64%. Laths of cumulus plagioclase are normally zoned with cores of An₆₂ and rims of An₄₈. They are cloudy, containing minute inclusions of spinel, especially in the cores. Intercumulus clinopyroxene has an augitic composition, En_{42–46}Fs_{10–12}Wo_{48–41}.

Simplified, coronas between olivine and plagioclase in this sample consist of an inner shell almost entirely composed of enstatite-rich orthopyroxene and an outer shell of pargasitic amphibole (Fig. 3). In detail, the actual situation may be more complex. The inner shell consists of columnar orthopyroxene grains, radially arranged around olivine, in a low-angle boundary (l.a.b.) arrangement manifested by undulatory extinction

(cf. Joesten 1986). Occasionally, the l.a.b. orthopyroxene has recrystallised into a granular fabric. The inner shell has a width between 26 and 93 μm. The width of the inner shell may vary by as much as 40 μm in a single corona but this variation is typically ~15 μm. Contacts between olivine and orthopyroxene are convex towards olivine (Figs. 4 and 5), indicating that orthopyroxene grew at the expense of the latter. Occasionally, contacts are cusped, with cusps ~5 μm wide and 7 μm deep, relative to a 50-μm local width of the orthopyroxene inner shell (Fig. 4). In the outer margin of the inner shell, rare, isolated inclusions of spinel occur (Figs. 4 and 5). These may be up to 20 μm in length. L.a.b. orthopyroxene ranges in composition from En₆₇ to En₇₁ with X_{Mg} values which are identical to those for exsolved orthopyroxene blebs, but higher than X_{Mg} values for bordering olivine (Table 1).

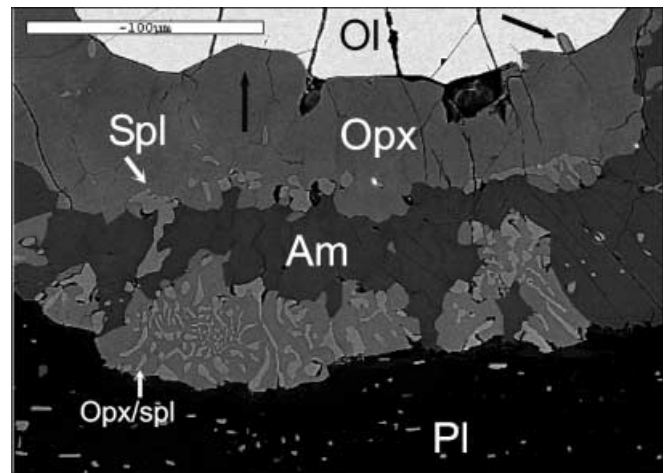


Fig. 4. SEM picture of an olivine–plagioclase corona, consisting of an inner shell of orthopyroxene with some isolated spinel inclusions, bordered by an outer shell of amphibole with inclusions of orthopyroxene–spinel symplectites. Note the convex and cusped contacts between olivine and orthopyroxene (filled arrows to the left and right respectively), and the fan-like shape of the orthopyroxene–spinel symplectites which stop halfway in the outer shell (for mineral abbreviations, see Fig. 2)

Table 2. Whole-rock and mineral REE contents and Sm–Nd isotopic compositions (*dl* below detection limit value)

	La ^a (ppm)	Ce (ppm)	Nd (ppm)	Sm (ppm)	Eu (ppm)	Tb (ppm)	Yb (ppm)	¹⁴⁷ Sm/ ¹⁴⁴ Nd	¹⁴³ Nd/ ¹⁴⁴ Nd
Whole rock	4.2	10.7	7.27	1.97	0.74	0.28	1.21	0.1640	0.512496 ± 4
Clinopyroxene	1.6	7.2	9.04	3.44	1.00	0.9	2.9	0.2303	0.513022 ± 4
Plagioclase I ^b	5.3	7.9	2.55	0.32	1.21	0.028	0.024	0.0752	0.511795 ± 7
Plagioclase II	3.63	6.1	2.08	0.30	1.19	0.03	0.10	0.0864	0.511885 ± 4
Plagioclase III	4.6	7.9	2.42	0.41	1.12	0.05	0.14	0.1011	0.511994 ± 6
Olivine	dl	dl	0.02	0.05	dl	dl	dl		
Orthopyroxene	1.04	1.2	1.61	0.47	0.17	0.15	0.5	0.1774	0.512594 ± 4
Amphibole	9.0	20	22.44	6.46	2.30	1.29	4.65	0.1739	0.512551 ± 5

^aLa, Ce, Eu, Tb and Yb determined by INAA, Nd and Sm by isotope dilution

^bPlagioclase I: 2.68–2.70 g/cm³ density fraction, plagioclase II: 2.70–2.72 g/cm³ density fraction, plagioclase III: density larger than 2.72 g/cm³

The outer shell is dominated by calcic amphibole which may either have an l.a.b. type of microstructure or display a granular, polygonal fabric. It has a pargasitic composition with X_{Mg} values between 0.69 and 0.71 and a compositional range $(Na_{0.63-0.74}K_{0.17-0.28})_{0.88-0.96}(Ca_{1.83-1.91}Na_{0.02-0.11}Fe_{0.05-0.13})_{2.00}(Fe_{1.04-1.18}Mn_{\leq 0.03}Mg_{2.83-3.04}Cr_{\leq 0.01}Ni_{0.01}Ti_{0.07-0.17}^{VI}Al_{0.71-0.97})_{5.00}(^{IV}Al_{1.86-1.97}Si_{6.03-6.14})_{8.00}O_{22}(OH)_2$. The width of the outer shell varies from 20 to 103 μm , although variation in a single corona is typically much less. In contrast to most olivine-plagioclase coronas described in the literature, the corona amphibole is not symplectitically intergrown with spinel. Isolated inclusions of orthopyroxene occur in the amphibole. This orthopyroxene has a slightly more Fe-rich composition than the inner shell orthopyroxene (Table 1). In several coronas (but not in all), fan-like orthopyroxene + spinel symplectites are present (Figs. 4 and 6). Hercynitic spinel in the symplectites, with Cr_2O_3 contents typically less than 0.10 wt% and X_{Mg} ranging from 0.43 to 0.50, is generally worm-like with a width up to 7 μm , and typically less. In some cases, spinel in the symplectites is granular, which may be due to recrystallisation during cooling. The fan-like symplectites widen towards the outer shell – plagioclase contact (Figs. 4 and 6). They are always in contact with the outer margin of the outer shell, and may either continue to the inner-outer shell contact (i.e. the amphibole shell itself may be discontinuous; Fig. 6) or stop halfway in the outer shell (Fig. 4). Where orthopyroxene + spinel symplectites are in contact with inner shell orthopyroxene, contacts are planar (Fig. 6). Outer shell – plagioclase contacts are generally convex towards plagioclase, irrespective of whether plagioclase is bordered by pargasitic amphibole or by orthopyroxene + spinel symplectite.

In a few odd coronas, clinopyroxene + spinel symplectite has been encountered in a similar arrangement

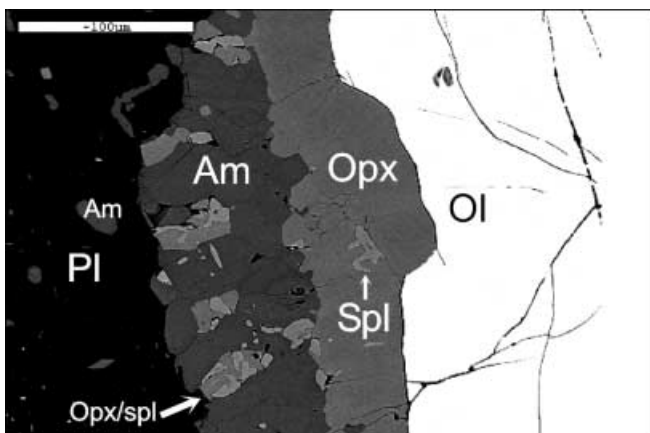


Fig. 5. SEM picture of a corona for which the outer shell largely consists of amphibole. The inner shell orthopyroxene contains some isolated spinel inclusions. Note the large cusp at the olivine-orthopyroxene interface, a result of partial consumption of olivine during formation of orthopyroxene (for mineral abbreviations, see Fig. 2)

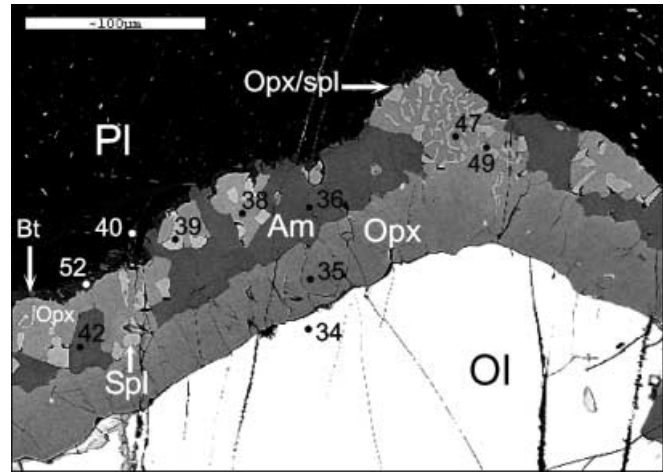


Fig. 6. SEM picture of a corona in which a fan-shaped orthopyroxene + spinel symplectite is in direct planar contact with the inner shell of orthopyroxene. Amphibole forms a discontinuous outer shell (for mineral abbreviations, see Fig. 2)

as, and adjacent to orthopyroxene + spinel symplectite (Fig. 7). This clinopyroxene is compositionally indistinguishable from intercumulus clinopyroxene except for its lower TiO_2 contents (Table 1). In a few cases, SEM and microprobe investigations revealed the occurrence of a very thin rim ($< 6 \mu m$) of biotite with composition $(K_{1.57}Na_{0.17}Ca_{0.08})_{1.82}(Fe_{1.14}Mg_{4.08}Ni_{0.02}Ti_{0.01}^{VI}Al_{0.66})_{5.91}(^{IV}Al_{2.37}Si_{5.63})_{8.00}O_{20}(OH)_4$ surrounding the outer shell of some coronas. No coronas are present between olivine and clinopyroxene. In cases where an original plagioclase-olivine boundary was apparently truncated by intercumulus clinopyroxene, the corona shells developed between the former minerals are discontinuous. However, a layer of orthopyroxene may occasionally (but not always) be present between olivine and intercumulus clinopyroxene.

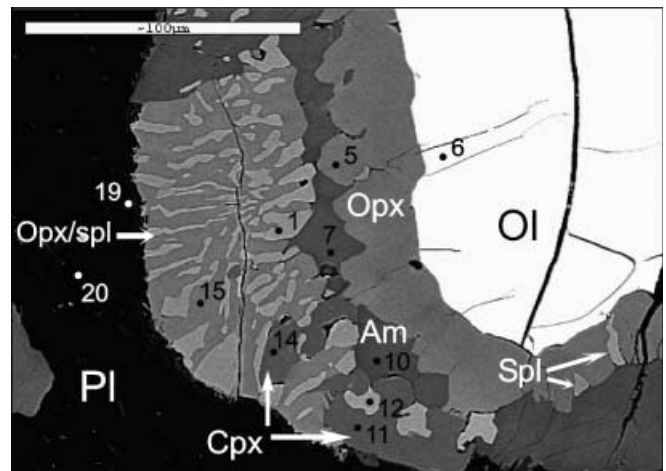


Fig. 7. An example of an odd corona in which, adjacent to the common orthopyroxene-spinel symplectites, clinopyroxene-spinel symplectites are observed (for mineral abbreviations, see Fig. 2)

Sm–Nd isochron calculations

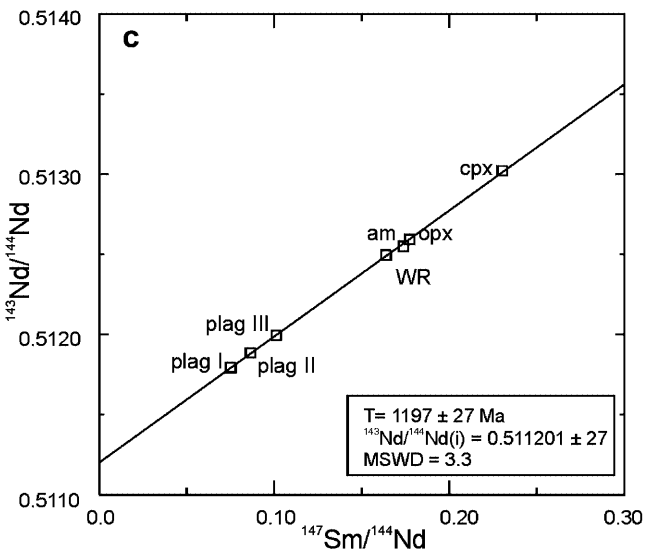
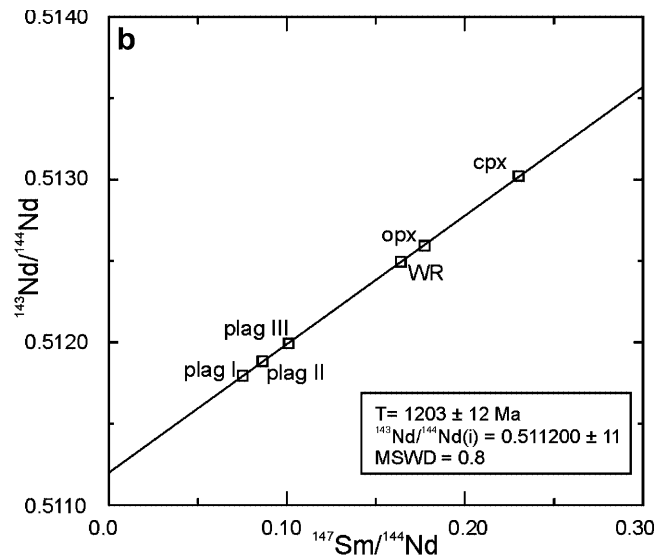
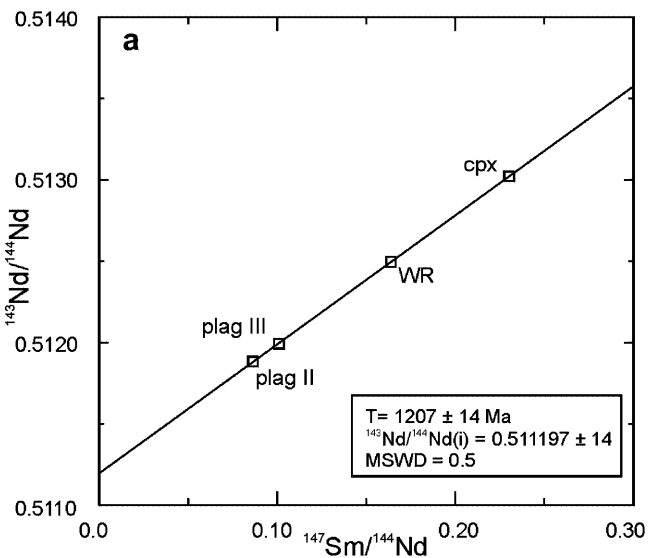
The intrusion age of the Vestre Dale gabbro may be calculated from the magmatic minerals, viz. plagioclase (fractions II and III) and clinopyroxene, and the whole-rock sample. As plagioclase shows normal zonation, i.e. a decrease of An content and hence in density from core to rim, it is assumed that these fractions represent parts of the plagioclase which have not been affected by corona formation or later processes. The resulting isochron age of $1,207 \pm 14$ Ma (MSWD = 0.5; Fig. 8a) is, within error, identical to the Sm–Nd whole-rock age of 1.11 ± 0.14 Ga for the Vestre Dale gabbro (de Haas et al. 1993). The dominance of olivine and plagioclase as cumulus phases causes a limited range in the $^{147}\text{Sm}/^{144}\text{Nd}$ ratios among the different cumulate groups (from 0.1618

to 0.1761; de Haas et al. 1993), resulting in a whole-rock isochron age with a relatively large uncertainty. $^{147}\text{Sm}/^{144}\text{Nd}$ ratios for the Sm–Nd whole rock – mineral isochron span a range between 0.0864 and 0.2303, allowing for a more precise age determination.

The $1,207 \pm 14$ Ma age compares well with ages reported for coronitic gabbros from the Kongsberg sector (Fig. 1), which has been argued to have formed one continuous belt with the Bamble sector during the mid-Proterozoic (Bugge 1943; Starmer 1990). Jacobsen and Heier (1978) presented a Rb–Sr whole-rock age of $1,200 \pm 50$ Ma (recalculated with $\lambda^{87}\text{Rb} = 1.42 \cdot 10^{-11} \text{a}^{-1}$) for the Vinoren gabbro. Munz and Morvik (1991) obtained a $1,224 \pm 15$ Ma Sm–Nd whole rock – plagioclase – clinopyroxene age for the Morud gabbro.

Regression of the magmatic assemblage, plagioclase fraction I and orthopyroxene yields an indistinguishable isochron age of $1,203 \pm 12$ Ma (MSWD = 0.8; Fig. 8b). The near-unity MSWD indicates isotopic equilibrium between the magmatic assemblage, orthopyroxene and

Fig. 8a–c. Sm–Nd isochron diagrams: **a** magmatic assemblage (cpx–plag II + III–WR), **b** magmatic assemblage + opx + plag I, and **c** magmatic assemblage + opx + plag I + am



plagioclase I. Regression including amphibole results in a comparable isochron age of $1,197 \pm 27$ Ma (Fig. 8c). Although the significantly higher MSWD value of 3.3 indicates that the scatter is beyond that which can be accounted for by analytical error, the growth of the corona minerals apparently took place before the main peak of Sveconorwegian metamorphism between 1,150 and 1,100 Ma.

REE modelling

Sm–Nd isotope systematics support a (partly) magmatic origin for the corona. Hence, it should be verified if systematics of the entire REE group within primary igneous and corona minerals in the Vestre Dale gabbro are in agreement with such a origin. A remarkable aspect of these REE systematics concerns their contents in corona orthopyroxene. Textural relationships indicate that orthopyroxene grew at the expense of olivine. A subsolidus origin for the orthopyroxene shell (e.g. Nishiyama 1983; Mongkoltip and Ashworth 1983), in which orthopyroxene largely grows at the expense of olivine (Grant 1988), however, cannot explain the observed REE budget of Vestre Dale inner shell orthopyroxene: orthopyroxene has much higher REE contents than olivine. Similarly, it is not possible to account for the REE abundances in corona amphibole by mass balance calculations based on any closed-system reaction (except for water) involving igneous plagioclase and olivine and corona orthopyroxene. The REE contents of the latter minerals are too low (Table 2). K contents in amphibole also indicate involvement of another component, as the orthoclase component in neighbouring plagioclase is less than 1% (Table 1). Residual magmatic liquids may be a candidate for such a component, and their interactions with already crystallised primary igneous minerals (olivine, plagioclase) should be considered. The composition of the parental magma of the Vestre Dale gabbro is not known but the REE abundances of cumulus plagioclase reveal that the REE abundances of the parental magma are not high enough to explain those of orthopyroxene and amphibole, given their mutual mineral/melt partition coefficients. Progressive crystallisation in a closed cumulus-intercumulus system, however, will raise abundances of incompatible elements like the rare earths in a fractionating magma. Such a fractionated liquid would explain the high REE abundances in corona orthopyroxene and amphibole.

Fractionation of the Vestre Dale magma started with crystallisation of olivine and plagioclase. The total REE budget is made up by plagioclase and the intercumulus liquid (the contribution of olivine is neglected, given its very low REE contents):

$$\sum REE = M_{\text{plag}} * c_{\text{plag,REE}} + M_{\text{IC}} * c_{\text{IC,REE}}$$

where $\sum REE$ = REE budget of the system, equivalent to the whole rock abundances (Table 2), M_{plag} = mass

fraction of plagioclase, $c_{\text{plag,REE}}$ = concentration of REE in plagioclase (Table 2), M_{IC} = mass fraction of intercumulus liquid, and $c_{\text{IC,REE}}$ = concentration of REE in intercumulus liquid.

As M_{plag} and M_{IC} are 39 and 26% respectively (determined by modal analysis), $c_{\text{IC,REE}}$ may be calculated (Table 3). As most of the intercumulus space is now occupied by clinopyroxene, its REE contents provides a check to the validity of this approach. REE contents of clinopyroxene should correspond to those in the intercumulus liquid using correct cpx/melt partition coefficients. Indeed, REE pattern and contents of clinopyroxene in WT217 are generally compatible with those of the calculated clinopyroxenes (Fig. 9a).

REE contents of the intercumulus liquid at this stage are still too low to account for those in corona orthopyroxene and amphibole. However, continued crystallisation of clinopyroxene will enhance the REE contents of the remaining intercumulus liquid, i.e. the final liquid, as REE clinopyroxene/melt distribution coefficients are significantly < 1 . REE abundances in the final liquid may be calculated according to:

$$c_{\text{FL,REE}} = \{c_{\text{IC,REE}} - (F_{\text{cpx}} * c_{\text{cpx,REE}})\} / (1 - F_{\text{cpx}})$$

where $c_{\text{FL,REE}}$ = concentration of REE in the final liquid, $c_{\text{IC,REE}}$ = concentration of REE in the intercumulus liquid, F_{cpx} = mass fraction of intercumulus liquid which crystallised into clinopyroxene, and $c_{\text{cpx,REE}}$ = concentration of REE in clinopyroxene (Table 2).

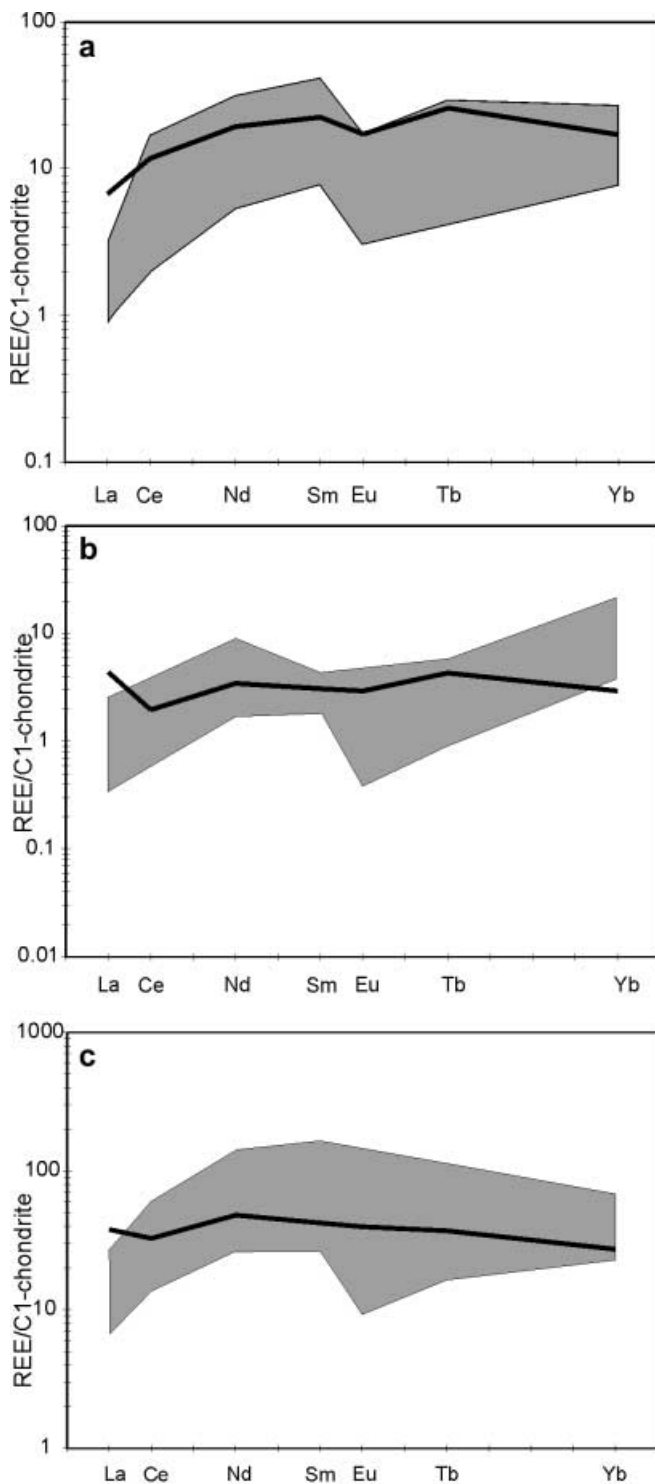
Results for $F_{\text{cpx}} = 0.8$ are presented in Table 3. REE concentrations in orthopyroxene and amphibole in equilibrium with this final liquid may be calculated using appropriate distribution coefficients. These calculations demonstrate that the REE concentrations in the final liquid have been sufficiently raised to account for the magnitude of REE contents in corona orthopyroxene and amphibole (Fig. 9b, c). Chondrite-normalised REE patterns of both corona orthopyroxene and amphibole show, however, some differences with the calculated

Table 3. Results of REE modelling (concentrations in ppm)

	Stage 1 ^a			Stage 2 ^b	
	(WR)	(plag)	(IC)	(cpx)	(final)
La	4.2	4.5	9.4	1.6	40.6
Ce	10.7	7.0	30.7	7.2	124.5
Nd	7.27	2.30	24.51	9.04	86.40
Sm	1.97	0.35	7.05	3.44	21.50
Eu	0.74	1.16	1.11	1.00	1.53
Tb	0.28	0.04	1.02	0.9	1.48
Yb	1.21	0.05	4.58	2.9	11.29

^aStage 1: composition of the trapped, intercumulus liquid (IC) after cumulus crystallisation of plagioclase (plag, average of all fractions). Composition of cumulus and intercumulus material is equivalent to whole-rock abundances (WR)

^bStage 2: composition of the fractionated final liquid (final) after 80% crystallisation of WT217 cpx (cpx) from the intercumulus liquid (IC)



patterns. Corona orthopyroxene lacks the steep HREE part of the pattern shown by calculated orthopyroxene compositions and has high La contents compared to Ce, whereas calculated orthopyroxene compositions show opposite behaviour (Fig. 9b). Corona amphibole lacks the negative Eu anomaly and moderately steep increase from La to Nd shown by (nearly) all calculated amphibole patterns (Fig. 9c).

Fig. 9a-c. Actual (measured) REE patterns (thick line) and calculated patterns (shaded fields) for **a** clinopyroxene, **b** orthopyroxene, and **c** amphibole. The calculated REE patterns assume crystallisation of clinopyroxene from an intercumulus liquid (*IC* in Table 3) and crystallisation of the orthopyroxene and amphibole from a fractionated intercumulus liquid, i.e. after 80% crystallisation into clinopyroxene (*final* in Table 3). Calculated patterns were obtained by applying different melt/mineral K_D values from the literature: Schnetzler and Philpotts (1970), Weill and McKay (1975), Henderson (1982), McKay (1982), Irving and Frey (1984), Budahn and Schmitt (1985), McKay et al. (1986), Hart and Dunn (1993), Johnson (1994), Sisson (1994), Dalpé and Baker (1994). C1-chondrite data from Sun and McDonough (1989)

These differences may in part be attributed to contemporaneous crystallisation of intercumulus phases other than clinopyroxene, such as zircon and apatite, both present in the Vestre Dale gabbro. Zircon preferentially incorporates HREE (Fujimaki 1986), resulting in a lower HREE budget of the final liquid. This will result in lower HREEs in orthopyroxene and amphibole, as is observed (especially for orthopyroxene; Fig. 9b). Apatite, on the other hand, tends to incorporate preferably the LREEs (e.g. Lieftink et al. 1994), which would lower rather than enhance the LREE contents, in contrast to the observations (Fig. 9b, c). Summarising, both Sm–Nd isotope systematics and REE chemistry require corona formation by interactions between primary igneous minerals and magmatic residual liquids.

Corona growth: magmatic and post-magmatic processes

Stage 1: Magmatic corona orthopyroxene formation

Sm–Nd isotope data, SEM observations, and REE modelling all demonstrate a magmatic origin for corona orthopyroxene.

1. Orthopyroxene is in isotopic equilibrium with plagioclase and clinopyroxene, both magmatic phases. The results of isochron calculations with and without orthopyroxene point towards contemporaneous crystallisation of plagioclase and clinopyroxene and corona orthopyroxene.
2. The REE budget of orthopyroxene is only explained by a significant contribution from fractionated magma (final liquid). Silica required for the replacement of olivine by orthopyroxene will also have been provided by this final liquid, as continued fractionation of a basic magma is accompanied by an increase of the silica content (cf. Naslund 1989).
3. SEM observations show that olivine-orthopyroxene contacts are convex towards olivine and locally strongly cusped, demonstrating formation of the orthopyroxene layer by reaction involving (partial) dissolution of olivine instead of solid-state diffusion.
4. The coexistence of both stable plagioclase-olivine contacts and coronitic microstructures on thin-section scale (e.g. Nijland et al. 1996). Formation of the

corona will be limited by the local availability of fractionated magma. The absence of sufficient fractionated magma in the intercumulus spaces, e.g. in case of an adcumulate-textured (part of the) rock, will prevent corona development.

Stage 2: Orthopyroxene + spinel symplectites

Inner shell l.a.b. orthopyroxene is occasionally in contact with outward-fanning orthopyroxene + spinel symplectites, in which case they have planar contacts (Fig. 6). This indicates a stable arrangement rather than growth at expense of another. The occurrence of orthopyroxene + spinel symplectites in olivine-plagioclase coronas has previously been described by Joesten (1986) in a sample of troctolitic gabbro from Risør in the Bamble sector, 40 km NE of the Vestre Dale gabbro. These coronas, displaying the sequence Ol | l.a.b. Opx | Opx + Spl symplectite | Am + Spl symplectite | Pl, have been interpreted as 'primary coronas' by Joesten (1986). In both these and the Vestre Dale coronas, the opx + spl symplectites show an outward growth direction. The orthopyroxene + spinel symplectites in the Risør sample separate an inner shell of l.a.b. orthopyroxene from a layer of amphibole + spinel symplectite (Joesten 1986, p. 445) whereas in the Vestre Dale sample, the symplectites do not occur in any kind of layer-like arrangement; they are not always in contact with inner shell orthopyroxene and do not separate an outer shell of calcic amphibole symplectitically intergrown with spinel. Risør orthopyroxene + spinel symplectites are considered to have developed at least in part contemporaneously with amphibole + spinel symplectite (Joesten 1986). In the case of the Vestre Dale gabbro, textures imply nucleation of orthopyroxene + spinel symplectites at the outer margin of the inner shell, followed by relatively rapid outward growth of the symplectites, and their subsequent replacement by calcic amphibole which started at the original outer shell – plagioclase interface. In solid state, such nucleation and outward fanning is restrained by the surrounding solid phases, whereas it is easily achieved in (and typical for) a saturated liquid. The lower X_{Mg} value of symplectitic orthopyroxene (Table 1) supports the concept of a stepwise growth, i.e. orthopyroxene crystallisation from a more fractionated magma than the inner shell orthopyroxene.

A similar origin may be proposed for clinopyroxene/spinel symplectites locally present. Inward growth of amphibole is supported by its locally preserved l.a.b. arrangement more or less perpendicular to the contact with plagioclase. The fact that orthopyroxene + spinel symplectites are locally absent may indicate their entire consumption or dissolution.

Stage 3: Post-magmatic formation of corona amphibole

Appearance of outer shell calcic amphibole constitutes the final stage of corona formation. The omnipresence

of relic orthopyroxene inclusions in this outer shell amphibole shows that formation of the corona shells consists of a series of reactions rather than the entire corona being the product of a single-stage process. Amphibole has largely grown at the expense of a pre-existing orthopyroxene layer instead of plagioclase (e.g. Grant 1988). Involvement of plagioclase is likely in the formation of amphibole in the Vestre Dale corona, and would explain the absence of the negative Eu anomaly in the amphibole REE pattern (Fig. 9c). It is, however, difficult to establish with certainty and to what extent.

The relationship between calcic amphibole and orthopyroxene + spinel symplectites in the outer shell is more difficult to interpret. The latter always occur at the contact between the outer shell and plagioclase, whereas amphibole is occasionally present between these symplectites and inner shell orthopyroxene. It may be proposed that the symplectites do not belong to the original corona, but developed by virtue of later dehydration (e.g. Dam 1995). If this is the case, it may be expected that orthopyroxene would (1) nucleate at the crystal faces of orthopyroxene already present, and (2) develop at places where a_{H_2O} was lowest, which is more likely at the contact between the inner and outer shells of the corona than at its outer margin, neither of which is observed. If it is assumed that the symplectites are due to post-corona dehydration and started at the outer shell – plagioclase interface, then the direction of growth of the symplectites should be inwards. This is at odds with the observed geometry of the orthopyroxene + spinel symplectites, whose fan-like internal arrangement indicates that they grew outwards.

Outer shell amphibole is apparently not in isotopic equilibrium with orthopyroxene and the igneous minerals. It may be argued that this is due to the fact that the Sm–Nd closure temperatures for amphibole are lower than those of the other minerals. Foden et al. (1995) indicated Sm–Nd closure temperatures of 500–650 °C for hornblende-garnet pairs. If corona amphibole underwent isotopic exchange until lower temperatures than the other minerals, an additional phase, such as a fluid, is required to re-equilibrate with. Growth of amphibole in an otherwise anhydrous mineral assemblage requires the intervention of an aqueous fluid anyway. Involvement of such a fluid would also help to explain the observed deviations from a purely magmatic REE pattern (Fig. 9c).

The partial replacement of orthopyroxene in the corona by amphibole, and relationships with orthopyroxene + spinel symplectite may be put forward as an argument in favour of growth of the amphibole during (Sveconorwegian) metamorphism. The transformation of the gabbro along the margin to garnet amphibolites makes it clear that the gabbro, or at least parts of the intrusion, has been exposed to relatively high-grade metamorphic conditions. Sm–Nd isochron calculations, however, (apparently) invalidate this option. It is highly unlikely that amphibolite facies metamorphism,

accompanied by the infiltration of hydrous fluids, would only affect the corona orthopyroxene, and would not result in the formation of any amphibole at the expense of intercumulus clinopyroxene or otherwise destruction of igneous textures. A metamorphic origin for the corona amphibole is excluded.

Magmatic fluids, remaining active during isobaric cooling after crystallisation of the gabbroic magma, are the most likely candidates to be involved in amphibole development. Generally, the water content of a differentiating magma increases with progressive fractionation. In the Vestre Dale gabbro, the width of the amphibole outer shell increases with increasing differentiation, from less than 50 μm in the troctolitic gabbros to more than 100 μm in the olivine-poor gabbros. This increase likely reflects the progressively water-rich nature of the magma, and as such argues for the involvement of late-stage magmatic fluids in the formation of the amphibole outer shell. Pure magmatic fluids, however, do not satisfactorily explain the enhanced La (and possibly also alkali) content of the amphibole, which requires input from an LREE-enriched source. The enhanced La and alkali contents are obviously due to contamination of the differentiating magma by a crustal component. The transition from troctolitic gabbros to ferrogabbros in the Vestre Dale gabbro is attended by an increase of the Sr isotope composition of the respective whole-rock samples, revealing continuous contamination of the differentiating magma, albeit on a rather restricted scale (de Haas et al. 1992). The most likely contaminating agent is the surrounding migmatitic gneiss. This gneiss is significantly more enriched in LREEs than the Vestre Dale gabbro (and its parental magma; de Haas, unpublished data); admixture of the parental magma, or the final liquid, with a gneiss-derived agent, such as an aqueous fluid, will result in the enhanced La concentration of the outer shell amphibole compared to calculated amphibole compositions.

Implications for lower crustal metamorphism

It is shown that corona development in the Vestre Dale gabbro is due to the interaction of the crystallised phases with late-stage magmatic liquids and, finally, fluids. Gabbroic intrusions in the Bamble sector commonly show irregular amphibolitisation in the inner parts of these intrusions, which cannot be explained by regional metamorphism. Likely, this type of amphibolitisation is also due to interaction with the similar late magmatic fluids. Intrusion of the Vestre Dale gabbro predates peak regional Sveconorwegian metamorphism in the Bamble sector (e.g. Kullerud and Dahlgren 1993). The post-magmatic stage of intrusions like the Vestre Dale gabbro in fact marks the beginning of Sveconorwegian metamorphism in the area. The conspicuous association of carbonic fluids with gabbroic intrusions in the Bamble sector (Touret 1986), which have also

been observed in samples from the Vestre Dale gabbro (Touret, personal communication 2001) indicates that the tandem of lower crustal intrusions and related fluids may be an essential part of triggering regional lower crustal granulite facies metamorphism in the area. The involvement of an aqueous La, K-bearing fluid in the development of outer shell amphibole indicates that low-salinity brines may also be part of this tandem, like in anorthosite-mangerite-charnockite-granite-type rocks (cf. Safonov 1999).

Conclusions

The results of this combined REE, SEM, and Sm–Nd isotope study provide strong arguments for a magmatic origin of the olivine-plagioclase coronas in the Vestre Dale gabbro:

1. inner shell corona orthopyroxene is in isotopic equilibrium with cumulus plagioclase and intercumulus clinopyroxene;
2. the REE contents of this corona orthopyroxene and amphibole, which is located in the outer shell, can be explained by a significant contribution of highly fractionated liquid, located in the intercumulus spaces;
3. SEM observations indicate formation of the corona orthopyroxene layer by reaction involving (partial) dissolution of olivine.

These findings are not compatible with the subsolidus, solid-state origin commonly proposed for olivine-plagioclase coronas. Such a model can not account for the REE contents of the corona orthopyroxene and amphibole, as the REE contents of the original phases in such a model, plagioclase and olivine, are too low. Moreover, SEM observations of the outer shell reveal that the corona is the product of a multistage process.

Development of the amphibole outer shell probably occurred by inward reaction, consuming the precursory outer shell of orthopyroxene + spinel symplectite. As formation of late amphibole at the expense of intercumulus clinopyroxene is entirely lacking, late-stage magmatic overgrowth is favoured over a metamorphic origin, whereas the slightly deviating REE and Sm–Nd characteristics of amphibole are explained by minor assimilation with increasing fractionation of the final liquid.

Acknowledgements The authors would like to thank Joep Huijsmans as one of the initiators of this study. Lodewijk IJlst kindly assisted with preparation of the mineral separates, and Coos van Belle and Piet Remkes with chemical preparation of these separates. Turid Winje and Muriel Erambert are acknowledged for technical assistance with SEM and microprobe respectively. A critical review by Lew Ashwal is greatly appreciated. Jacques Touret is thanked for his editorial handling of the manuscript and for his stimulating advice which led to a considerable improvement of the original manuscript. One of the authors (GJH) acknowledges financial support of the European Union (Contract ERBF MBICT 950294).

References

- Adams FD (1893) Über das Norian oder Ober-Laurentian von Canada. *Neues Jahrb Mineral Beilageband* 8:466–470
- Ashworth JR (1986) The role of magmatic reaction, diffusion and annealing in the evolution of coronitic microstructure in troctolitic gabbro from Risør, Norway: a discussion. *Mineral Mag* 50:469–473
- Ashworth JR, Birdi JJ, Emmett TF (1992) A complex corona between olivine and plagioclase from the Jotun Nappe, Norway, and the diffusion modelling of multiminerale layers. *Mineral Mag* 56:511–525
- Bard JP (1986) *Microtextures of igneous and metamorphic rocks*. Reidel, Dordrecht, pp 1–261
- Becke F (1882) Die Gneissformation des niederösterreichischen Waldviertels. *Tscherm Mineral Petrol Mitt* 4:352–357
- Brickwood JD, Craig JW (1987) Primary and re-equilibrated mineral assemblages from the Sveconorwegian mafic intrusions of the Kongsberg and Bamble areas, Norway. *Nor Geol Unders Bull* 410:1–23
- Brogger WC (1934) On several Archean rocks from the south coast of Norway II. The South Norwegian hyperites and their metamorphism. *Skrift Norsk Videns Akad Matematisk-Naturvidens Kl* 1:1–421
- Bruin M de (1983) Instrumental neutron activation analysis – a routine method. PhD Thesis, Delft University of Technology
- Budahn JR, Schmitt RA (1985) Petrogenetic modelling of Hawaiian tholeiitic tholeiites: a geochemical approach. *Geochim Cosmochim Acta* 49:67–87
- Bugge JAW (1943) Geological and petrological investigations in the Kongsberg – Bamble formations. *Nor Geol Unders Bull* 160:1–150
- Dalpe C, Baker DR (1994) Partition coefficients for rare-earth elements between calcic amphibole and Ti-rich basaltic glass at 1.5 GPa, 1100 °C. *Mineral Mag* 58A:207–208
- Dam BP (1995) Geodynamics in the Bamble area during Gothian and Sveconorwegian times. PhD Thesis, Utrecht University
- Davidson A, Van Breemen O (1988) Baddeleyite-zircon relationships in coronitic metagabbro, Grenville Province, Ontario: Implications for geochronology. *Contrib Mineral Petrol* 100:291–299
- Foden J, Mawby J, Lelley S, Turner S, Bruce D (1995) Metamorphic events in the eastern Arunta Inlier, part 2. Nd-Sr-Ar isotopic constraints. *Precambrian Res* 71:207–227
- Frodesen S (1968a) Coronas around olivine in a small gabbro intrusion, Bamble area, south Norway. *Nor Geol Tidsskr* 48:201–206
- Frodesen S (1968b) Petrographical and chemical investigations of a Precambrian gabbro intrusion, Hiåsen, Bamble area, south Norway. *Nor Geol Tidsskr* 48:281–306
- Fujimaki H (1986) Partition coefficients of Hf, Zr, and REE between zircon, apatite, and liquid. *Contrib Mineral Petrol* 94:42–45
- Gardner PM, Robins B (1974) The olivine-plagioclase reaction: Evidence from the Seiland petrographic province, northern Norway. *Contrib Mineral Petrol* 44:149–156
- Grant SM (1988) Diffusion models for corona formation in metagabbros from the western Grenville Province, Canada. *Contrib Mineral Petrol* 98:49–63
- Grieve RAF, Gittins J (1975) Composition and formation of coronas in the Hadlington gabbro, Ontario, Canada. *Can J Earth Sci* 12:289–299
- Haas GJLM de (1992) Source, evolution, and ages of coronitic gabbros from the Arendal-Nelaug area, Bamble, southeast Norway. PhD Thesis, Utrecht University
- Haas GJLM de, Nijland TG, Huijsmans JPP, Maijer C, Dam BP (1992) The pre-corona history of a gabbroic intrusion in the Bamble sector, Vestre Dale, Norway. *Neues Jahrb Mineral Monatshefte*:221–240
- Haas GJLM de, Verschure RH, Maijer C (1993) Isotopic constraints on the timing of crustal accretion of the Bamble Sector, Norway, as evidenced by coronitic gabbros. *Precambrian Res* 64:403–417
- Hart SR, Dunn T (1993) Experimental cpx/melt partitioning of 24 trace elements. *Contrib Mineral Petrol* 113:1–8
- Henderson P (1982) *Inorganic geochemistry*. Pergamon, Oxford
- Hommel W (1919) *Grundzüge der systematische Petrographie auf genetischer Grundlage*. Berlin, vol I
- Irvine TN (1982) Terminology for layered intrusions. *J Petrol* 23:127–162
- Irving AJ, Frey FA (1984) Trace element abundances in megacrysts and their host basalts: Constraints on partitioning coefficients and megacryst genesis. *Geochim Cosmochim Acta* 48:1201–1221
- Jacobsen SB, Heier KS (1978) Rb-Sr isotope systematics in metamorphic rocks, Kongsberg sector, South Norway. *Lithos* 11:257–276
- Joesten R (1986) The role of magmatic reaction, diffusion and annealing in the evolution of coronitic microstructure in troctolitic gabbro from Risør, Norway. *Mineral Mag* 50:441–467
- Johnson KTM (1994) Experimental cpx/melt and garnet/melt partitioning of REE and other trace elements at high pressures: Petrogenetic implications. *Mineral Mag* 58A:454–455
- Korshinskij DS (1959) Physicochemical basis of the analysis of the paragenesis of minerals. Consultants Bureau, New York
- Kullerud L, Dahlgren S (1993) Sm-Nd geochronology of Sveconorwegian granulite facies mineral assemblages in the Bamble shear belt, south Norway. *Precambrian Res* 64:389–402
- Lacroix A (1889) Contribution à l'étude des gneiss à pyroxène et des roches à wernérites. *Bull Soc Fr Minéral* 12:83–350
- Lieftink DJ, Nijland TG, Maijer C (1994) The behaviour of rare-earth elements in high-temperature Cl-bearing aqueous fluids: results from the Ødegårdens Verk natural laboratory. *Can Mineral* 32:149–158
- Ludwig KR (1996) Isoplot, a plotting and regression program for radiogenic-isotope data, version 2.90. US Geol Surv Open-File Rep 91–445
- McKay G (1982) Experimental REE partitioning between pigeonite and Apollo 12 olivine basaltic liquids. *EOS* 63:1142
- McKay G, Wagstaff J, Yang SR (1986) Clinopyroxene REE distribution coefficients for shergottites: the REE content of the Shergotty melt. *Geochim Cosmochim Acta* 50:927–937
- Mongkoltip P, Ashworth JR (1983) Quantitative estimation of an open-system symplectite-forming reaction: Restricted diffusion of Al and Si in coronas around olivine. *J Petrol* 24:635–661
- Morton RD, Batey RH, O'Nions RK (1970) Geological investigations in the Bamble sector of the Fennoscandian Shield in south Norway I. The geology of eastern Bamble. *Nor Geol Unders Bull* 263:1–72
- Munz IA, Morvik R (1991) Metagabbros in the Modum complex, southern Norway: An important heat source for Sveconorwegian metamorphism. *Precambrian Res* 52:97–113
- Naslund HR (1989) Petrology of the Basistoppen sill, east Greenland: A calculated magma differentiation trend. *J Petrol* 30:299–319
- Nijland TG, Maijer C (1993) The regional amphibolite to granulite facies transition at Arendal, Norway: Evidence for a thermal dome. *Neues Jahrb Mineral Abh* 165:191–221
- Nijland TG, Maijer C, Haas GJLM de (1996) The Stokkafjell troctolite, SW Norway: Its bearing on the early p-T evolution of the Rogaland terrane. *Neues Jahrb Mineral Abh* 171:91–117
- Nishiyama T (1983) Steady diffusion model for olivine-plagioclase corona growth. *Geochim Cosmochim Acta* 47:283–294
- Reynolds RC, Frederickson AF (1962) Corona development in Norwegian hyperites and their bearing upon the metamorphic facies concept. *Geol Soc Am Bull* 73:1–59
- Rosenbusch H (1910) *Elemente der Gesteinslehre*. E Schweizerbart'sche, Stuttgart
- Safonov OG (1999) The role of alkalis in the formation of coronitic textures in metamangerites and metaanorthosites from the Adirondack complex, United States. *Petrology (Moscow)* 7: 102–121

- Schnetzler CC, Philpotts JA (1970) Partition coefficients of rare-earth elements between igneous matrix material and rock-forming mineral phenocrysts-II. *Geochim Cosmochim Acta* 34:331–340
- Schrauf A (1882) Beiträge zur Kenntnis des Associationskreises der Magnesia-Silikate. *Z Mineral Kristallogr* 6:359
- Sederholm J (1916) On synantectic minerals and related phenomena. *Bull Com Géol Finlande* 48:9–41
- Sisson TW (1994) Hornblende-melt trace-element partitioning measured by ion microprobe. *Chem Geol* 114:331–344
- Sjögren H (1883) Om de norska apatitförekomsterna och om sannolikheten att anträffa i Sverige. *Geol Fören Stockholm Förh* 6:447–498
- Starmer IC (1969) Basic plutonic intrusions of the Risør-Søndeled area, south Norway: The original lithologies and their metamorphism. *Nor Geol Tidsskr* 49:403–431
- Starmer IC (1985) The evolution of the south Norwegian Proterozoic as revealed by major and mega-tectonics of the Kongsberg and Bamble sectors. In: Tobi AC, Touret JLR (eds) *The deep Proterozoic crust in the North Atlantic Provinces*. NATO ASI Series vol C158. Reidel, Dordrecht, pp 259–290
- Starmer IC (1990) Mid-Proterozoic evolution of the Kongsberg-Bamble belt and adjacent areas, southern Norway. In: Gower CF, Rivers T, Ryan B (eds) *Mid-Proterozoic Laurentia-Baltica*. *Geol Assoc Can Spec Pap* 38:279–305
- Sun S-S, McDonough WF (1989) Chemical and isotopic systematics of oceanic basalts: implications for mantle composition and processes. In: Saunders AD, Norry MJ (eds) *Magmatism in the ocean basins*. *Geol Soc Lond Spec Publ* 42:313–345
- Törnebohm AE (1877) Om Sveriges viktigare diabas-och gabbroarter. *Svensk Vetensk-Akad Handlingar* B14
- Touret J (1986) Fluid inclusions in rocks from the lower continental crust. In: Dawson JB, Carswell DA, Hall J, Wedepohl KH (eds) *The nature of the lower continental crust*. *Geol Soc Lond Spec Publ* 24:161–172
- Turner SP, Stuewe K (1992) Low-pressure corona textures between olivine and plagioclase in unmetamorphosed gabbros from Black Hill, south Australia. *Mineral Mag* 56:503–509
- Valbracht PJ (1991) Early Proterozoic continental tholeiites from western Bergslagen, central Sweden. II. Nd and Sr isotopic variations and implications for the Svecofennian sub-continental mantle. *Precambrian Res* 52:215–230
- Vogt JHL (1921) The physical chemistry of the crystallization and magmatic differentiation of igneous rocks. *J Geol* 29:645–647
- Weill DF, McKay GA (1975) The partitioning of Mg, Fe, Sr, Ce, Sm, Eu, and Yb in lunar igneous systems and a possible origin of KREEP by equilibrium partial melting. In: *Proc 6th Lunar Sci Conf*, pp 1143–1158